WATER BALANCE AND INFILTRATION IN A SEASONAL FLOODPLAIN IN THE OKAVANGO DELTA, BOTSWANA

Lars Ramberg, Piotr Wolski, and Martin Krah
Harry Oppenheimer Okavango Research Centre
University of Botswana
P/Bag 285
Maun, Botswana

Corresponding author:
E-mail: pwolski@orc.ub.bw

Abstract: Water balance in a seasonal floodplain in the Okavango Delta, Botswana was determined for three years (1997–1999). There was no surface outflow, and infiltration to ground water was very large (4.7–9.7 m during 90–175 days of flooding, or on average 4.6–5.4 cm·d^{-1}), amounting to 90% of total annual loss of water from the floodplain. At the arrival of the flood, when floodplain ground water was 3–5 m below ground, infiltration was controlled by vertical percolation through the aeration zone and was taking place with rates as high as 1.11–1.74 m during 10 days, or on average 11.1–17.4 cm·d^{-1}. Lateral ground-water flow from the floodplain toward surrounding dryland became the dominant process after the first days of flooding, when the floodplain ground-water table rose to the surface. Lateral ground-water drainage accounted for at least 80% of total infiltration. Direct measurements of infiltration confirmed high rates obtained from the water balance and revealed that the majority of infiltration occurred within a 10-m belt along the shore of the inundated area, with point infiltration rates as high as 42 cm·d^{-1}. The infiltration values are high compared to other large recharge wetlands (e.g., the Everglades, the Hadejia-Nguru) and result from a combination of lack of a low permeability surface layer in the floodplain and strong drainage of floodplain ground water driven by evaporation from the surrounding drylands. High infiltration and lateral ground-water flows have major implications for the Okavango Delta ecology, as they provide water to riparian vegetation, affect floodplain nutrient balance, and are part of the process responsible for immobilization of dissolved minerals.

Key Words: water balance, infiltration, groundwater, flood, seasonal wetland, Okavango

INTRODUCTION

One of the hydrologic processes taking place in wetlands is the interaction of surface water (SW) and ground water (GW). Wetlands are generally linked to ground water; one can distinguish wetlands dominated by ground-water discharge, by ground-water recharge, and flow-through wetlands (Winter 1999, Mitsch and Gosselink 2000). The magnitude and direction of the SW-GW flux is important for two reasons. First, it affects biochemistry of the wetland (LaBaugh et al. 1987, Mitsch and Gosselink 2000) and particularly biological and biochemical processes occurring at the water-soil interface, or hyporheic zone (Brunke and Gonser 1997, Jones and Mulholland 2000). Surface water and ground water differ in such important physical and chemical characteristics as temperature, pH, redox potential, concentrations of oxygen, CO_2, nitrate, ammonium, and dissolved organic matter, and thus, the nature and magnitude of SW-GW fluxes strongly affect

the retention and metabolism of organic matter in this important wetland ecotone (Brunke and Gonser 1997). Second, the dynamics of the interactions between surface water and ground water determine the wetland's hydroperiod or the duration, extent, and depth of inundation, particularly for isolated wetlands (Mitsch and Gosselink 2000). Furthermore, SW-GW interactions cause the ground water in the vicinity of a wetland to be functionally related to the wetland itself, leading to an ecological framework where the dryland vegetation of the riparian zone is considered part of the wetland (Tiner 1999). The dynamics of SW-GW fluxes can affect the ecology of the riparian vegetation (Hughes 1990, Ringrose 2003) by determining availability and depth of ground water. On the other hand, riparian vegetation can influence wetland's hydrology through transpirative uptake of ground water (Sacks et al. 1992, Doss 1993, Winter and Rosenberry 1995), thus facilitating surface-water loss to ground water and reduction of a wetland's hydroperiod.

The nature of interactions between surface water and ground water (i.e., direction and magnitude of the water flux, and their seasonal variation) is the result of a complex interplay of climate, morphology, soils, geology, vegetation, and hydrology of a system, and thus varies widely among systems (Winter et al. 1998, Winter 1999, Woessner 2000, Sophocleous 2002). Below, we describe a few wetlands that bear some relevance to the topic of our paper.

SW-GW interactions of prairie pothole wetlands in glacial terrain of the northern U.S. and Canada are determined by factors affecting their link to the sub-regional ground-water system: geology (presence or lack of impermeable substratum) and topography (altitude of pothole bottom). Permanently inundated potholes are usually linked to regional ground water and receive ground-water discharge (Winter and Rosenberry 1995). Uptake of ground water for transpiration by fringing riparian vegetation might, however, cause temporary reversal of the direction of ground-water flow – the potholes that normally receive ground water might become ground water recharging ones (Winter and Rosenberry 1995). Seasonally inundated potholes are usually rain and snowmelt fed. Surface water in the potholes usually infiltrates to the ground, recharging shallow, sometimes perched, ground water. Average infiltration rates on the order of 1 cm·d^{-1} were observed by Hayashi et al. (1998). A large part of this infiltrating water is transferred laterally toward surrounding upland and used by fringing riparian vegetation, and only 2% contributes to deep ground-water recharge (Hayashi et al. 1998).

The Everglades wetlands in the U.S. are characterized by peaty substratum overlying highly permeable sand and karstic aquifer. Ground-water recharge and discharge alternate there in time, driven by the differential responses of surface water and ground water to precipitation events and operation of water-control structures (Choi and Harvey 2000, Harvey et al. 2000, Harvey et al. 2004). Ground-water recharge occurs during rising and high surface-water-level conditions, and discharge occurs during low and decreasing surface-water levels. In north-central Everglades studied by Harvey et al. (2004), where wetlands are compartmentalized by a system of dikes, levees, and canals, upward ground-water flux up to 6 cm·d^{-1} was observed in the wetland in the direct vicinity of elevated canals and was attributed to canal seepage and ground-water flow in local ground-water flow systems. In the vicinity of drainage canals, recharge rates up to 10 cm·d^{-1} were observed. In the central part of the "compartments," where driving forces for recharge and discharge by natural topographic gradients are small, recharge and discharged events were alternating, and net ground-water recharge of 11 cm·a^{-1} was observed. Harvey et al. (2004) suggested that this central part of the "compartment" reflects SW-GW interactions in the natural, pre-regulation state of that wetland.

In seasonally inundated alluvial plain wetlands that are usually present in broad valleys of meandering or braided rivers, SW-GW interaction is driven by floods. A general model of this interaction is outlined by Winter et al. (1998). During in-bank events, rising surface water recharges the alluvial aquifer by infiltration through channel banks, while vertical infiltration takes place during overbank floods. During flood recession, floodplain ground water discharges laterally to river channel. Several factors complicate this general pattern. Depending on the nature and permeability of floodplain deposits, vertical infiltration may be widespread within the floodplain, fast and quantitatively important (e.g., Harrington et al. 2002, Martí et al. 2000), or it may be an insignificant component of floodplain water balance and occur only locally (e.g., Jolly et al. 1994, Lamontagne et al. 2005). Local ground-water flow systems resulting from small topographic differences associated with terraces, oxbow lakes, etc., as well as regional ground-water flow systems originating in the surrounding uplands and discharging within the valley, may cause presence of patches differing in magnitude and direction of SW-GW flux (Winter et al. 1998).

In this paper, we describe the water balance of a seasonal floodplain in the Okavango Delta and the factors affecting its hydrology, with particular attention to the role of infiltration. In a broader sense, by this work, we provide a quantitative description of the water balance of a wetland system dominated by ground-water recharge, examples of which are few in the literature.

The Okavango Delta is the world's largest Ramsar site – a wetland of international importance. The Okavango Delta is a key element in the Botswana tourism industry (Mbaiwa 2003) and has great conservation value, as it creates an ecological "oasis" in the otherwise arid environment, supporting large numbers of wildlife in a landscape of extraordinary beauty. It is also the basis of subsistence of a large local population (Kgathi et al. 2005). The Okavango Delta is under development pressure resulting from water demand for domestic and agricultural purposes, demand for hydroelectricity, and management schemes such as channel clearing, in the Okavango Delta proper and in the Okavango River catchment (Turton et al. 2003). In
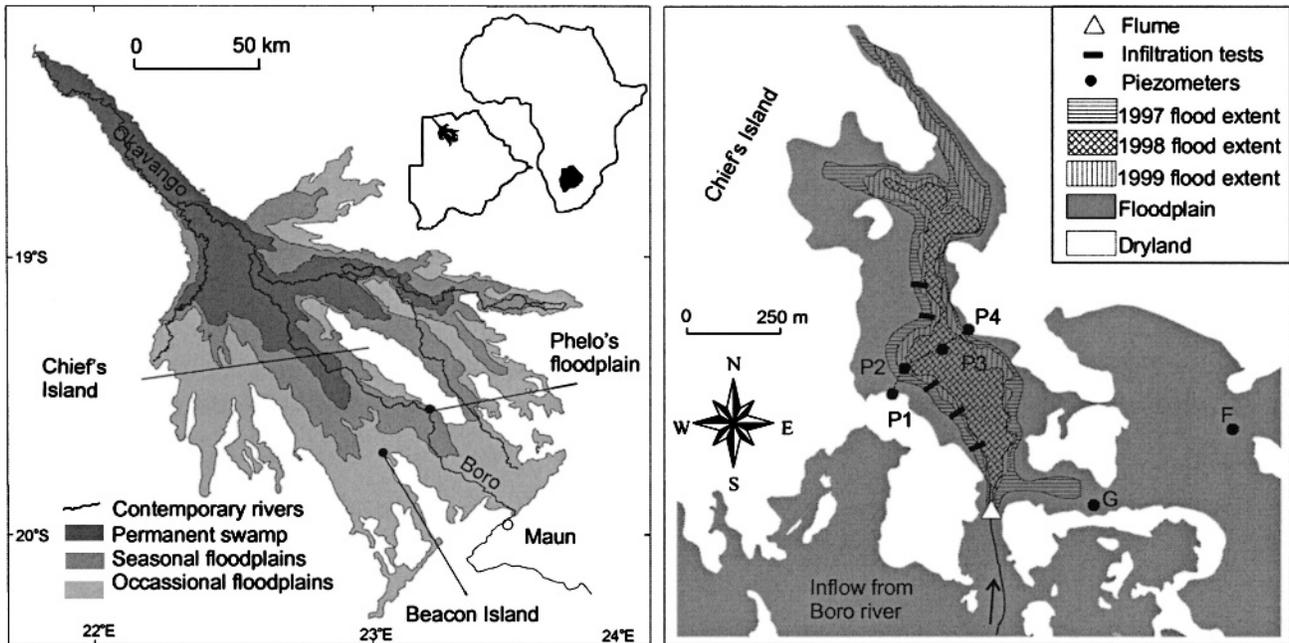
Figure 1.   Location map of the Okavango Delta and Phelo's floodplain.

this context, with this paper, we contribute to the understanding of the hydrologic and ecological functioning of the Okavango wetland, which is not only theoretically important but also crucial as the basis for wise management of the system. In particular, we provide a quantitative understanding of the role of infiltration in the seasonal floodplains of that system and factors affecting its seasonal dynamics. In this manner, we improve the basis for a wide range of on-going and future studies addressing spatial and temporal distribution and availability of nutrients (e.g., Mubyana et al. 2003), inorganic chemicals (e.g., Krah et al. 2005), and biologically important components such as DOC (e.g., Mladenov et al. 2005), leading to an understanding of food-web dynamics (e.g., Hoberg et al. 2002) in the seasonal floodplains of the Okavango Delta.

STUDY SITE

The Okavango Delta (Figure 1) is a large inland wetland created by the Okavango River. Its general hydrology has been often described in the literature (Dinçer et al. 1987, Gieske 1997, McCarthy et al. 1998). The principal hydrologic feature of the Okavango Delta is the seasonal flood arriving from the Okavango River catchment in Angola and, to a lesser extent, resulting from local rainfall. The area covered by water expands from its annual low of 2500–4000 km^2 in February-March to its annual high of 6000–12000 km^2 in August-September (McCarthy et al. 2004). The seasonality of in-

undation is the basis for distinguishing three major hydro-ecological zones: permanent swamp, seasonal (regularly flooded) floodplains, and occasional floodplains (Figure 1), which differ in vegetation cover and ecological functioning (SMEC 1989, Ellery and Ellery 1997). The flood cycle is out of phase with the rainy season, which occurs between November and March. Geomorphologicaly, the Okavango Delta is an alluvial fan, with 1:3600 longitudinal gradient (McCarthy et al. 1997). It is a mosaic of floodplains and islands of sizes varying from several square meters to 1000 km^2 (Gumbricht et al. 2003). The climate of the region of the Okavango Delta is semi-arid with 460 mm·a^{-1} of rainfall and one distinct rainy season from November to March. Class A pan evaporation (with an appropriate, seasonally-varying pan coefficient) amounts to 1800 mm·a^{-1}. Maximum monthly rates of 250 mm·month^{-1} occur in October and minimum of 90–100 mm·month^{-1} occur in June/July.

The floodplain studied here (Figure 1), hereafter called Phelo's Floodplain, is located between an unnamed island and the southwest edge of Chief's Island, one of the largest dry land bodies within the Okavango Delta. The floodplain area is about 0.4 km^2, and it has no surface outlet. It is connected to the Boro River, one of the main watercourses in the Okavango Delta, by a 1 km long, 20–30 m wide channel. The topographic relief of the area is very low, with maximum topographic variations of 2 m over distances of 3 km. The substratum is primarily made up of medium to fine sands and sandy loams
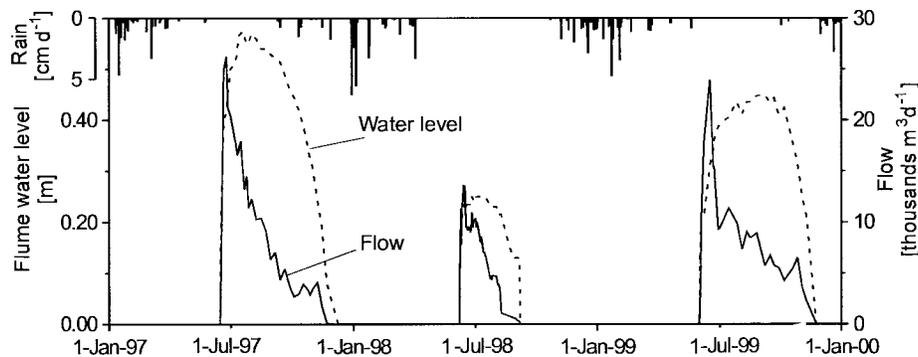
Figure 2.   Water level and inflow hydrographs for Phelo's floodplain.

and is characterized by high hydraulic conducti-vity: $1.2 \cdot 10^{-4}$–$3.5 \cdot 10^{-4}$ m·s^{-1} (Obakeng and Gieske 1997) and high infiltration capacity: $4.6 \cdot 10^{-4}$–$1.2 \cdot 10^{-3}$ m·s^{-1} (Boring and Björkvald 1999).

Phelo's Floodplain is characterized by distinct vegetation zoning, reflecting the topography, which accentuates differences in hydroperiod. The central, deeper part of the floodplain, annually flooded for 4–5 months or more, is vegetated by dense stands of *Cyperus articulatus* L. This is surrounded by a zone where inundation lasts 2–3 months, which is covered by heavily grazed grass, predominantely *Panicum repens* L. At the floodplain-riparian woodland fringe, where flooding occurs rarely and lasts not longer than 1–2 months, occur scattered stands of tall grasses such as *Imperata cylindrica* (L.) Raeuschel. The woodlands are stratified perpendic-ularly to the adjacent floodplain. The fringe hosts typically broad-leafed mainly evergreen trees such as *Croton megalobotrys* Muell. Arg., *Diospyros mespi-liformis* Hochst. ex A. DC., *Garcinia livingstonei* T. Anders. and *Ficus sycomorus* L. These give way gradually to *Acacia* spp. woodlands followed further inland by open dry woodland savanna, with typical species like *Colophospermum mopane* (Kirk ex Benth.) Kirk ex J. Leonard. An alternative zonation occurs to the west of the flume (Figure 1), when the soils inside the riverine fringe are salty. Salt-tolerant trees like the palm *Hyphaene petersiana* Klotzsch are found here followed further inland by open grass-land with higher salinities and specialist grasses like *Sporobolus spicatus* (Vahl.) Kunth. These vegetation sequences are characteristic of the entire seasonal floodplains zone of the Okavango Delta (Ellery et al. 1993).

METHODS

Measurements of Inflow

During the flooding phase, the inlet to Phelo's Floodplain becomes increasingly vegetated by dense stands of floating leaf and emergent macrophytes. However, the deepest central part, 1–3 meters wide, is kept more or less open by hippopotami moving in and out of the floodplain. The natural section could not be used for routine flow measurements, mainly due to the vegetated part being charac-terized by very low flow velocities (<0.01 m·s^{-1}). To measure the volume of in-flowing water, an earth dike and a concrete flume were constructed as a part of this study. The flume was constructed to coincide with the central, open part of the section, and its bottom elevation was kept at the natural level. The inflow was measured during 1997–1999 flood seasons at least once a week but in particu-lar at the arrival of the flood, often daily, by use of a current meter.

Floodplain Survey Data

The relationship between water volume stored in the floodplain and water level was obtained by constructing a hypsographic diagram from a digital elevation model (DEM). The DEM has a spatial resolution of 10 m and was based on a topographic map derived in an earlier study (Meyer 1999) from detailed ground survey using standard geodetic methods.

Calculations of the Water Balance

The water balance was calculated for 10-day intervals. Because the floodplain has no surface outlet and no rainfall was recorded during the flooding seasons of the studied years (Figure 2), the following simplified formula was used:

$$Q_I = E + I + \varDelta S \qquad (1)$$

where Q_I is surface inflow, E – evaporation from the area covered by water during the given period, I – infiltration to the ground (i.e., flux across the ground surface within the inundated area) and
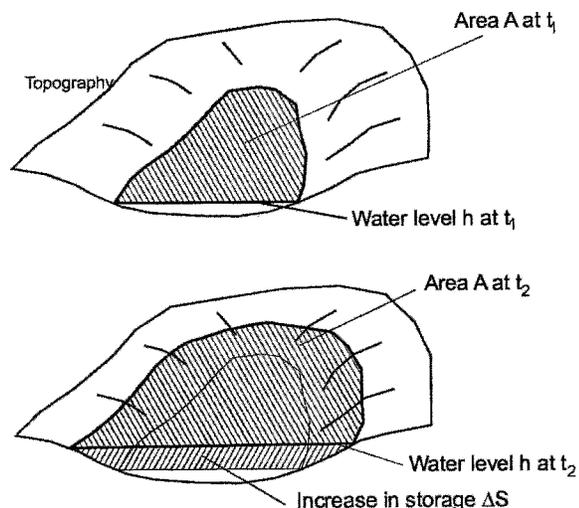
Figure 3. Scheme used in calculating water balances. Due to flatness of the area, the difference between horizontal surface A and topographic surface was considered negligible. Evapotranspiration and infiltration were calculated across the area A.

ΔS – change in floodplain storage above the ground surface (Figure 3).

It was assumed that the evapotranspiration from the area covered by water, E, was equal to that of an open water surface E_0. To estimate the latter, climatic data from the 53 km distant village of Maun (Figure 1) were used. SMEC (1987), based on the detailed water-balance study, adjusted coefficients of the Penman formula for open water evaporation presented by Doorenbos and Pruitt (1984) so specific climatic conditions of Botswana were reflected. In our study, we used the SMEC (1987) version of the Penman formula. The use of data from Maun was justified by the fact that there is little variation in climatic conditions between Maun and the seasonal floodplains zone of the Okavango Delta (UNDP/FAO 1977). These differences manifest themselves mainly by winter minimum daily temperatures being 1–2°C higher within the Okavango Delta than in Maun. This, when implemented in the Penman formulation, gives a difference in E_0 of less than 2.5%.

Sensitivity Calculations

Two of the water balance elements used for calculation of infiltration, i.e. evaporation and change in storage, are not directly measured but calculated from proxy data. Possible errors in determination of these variables influence the calculated value of infiltration. Assessment of effects of these errors on the calculated output can be done in the framework of uncertainty analysis (e.g. Choi

and Harvey 2000). This, however, demands that the errors in input variables are quantified. In our case the available data do not allow for realistic quantification of errors in input variables. For example, a topographic survey was not done within our study, and use was made of an existing topographic map (Meyer 1999), for which interpolation and survey errors were not known. The discussion by Mitsch and Gosselink (2000) indicates that the deviation of calculated rates from measured ones for evapotranspiration from wetlands rarely is larger than ± 20%, but no data exist to confirm this range in the Okavango. As a result, strict uncertainty analyses could not be performed. We have used sensitivity analysis instead, in which output (infiltration) was calculated for a wide range of input values. Floodplain storage and evaporation were increased and decreased by up to 50% with respect to their original values. In this way, we intended to visualize uncertainty of our water-balance model, avoiding arbitrary determination of errors in its inputs. The effects on infiltration were assessed through mean percent change in total annual infiltration and mean percent change in 10-day infiltration.

Ground-water Table Fluctuations

A number of shallow piezometers were installed within and around the floodplain before the first studied flooding season of 1997 (Figure 1). Piezometers were constructed using 50-mm PVC pipes installed to the depth of 3–6 m under ground using a hand auger and a bailer. The bottom section (3 m) of pipes was slotted, and the slotted section was isolated from the surface using bentonite pellets. Piezometer pipes protruded only 0.1–0.2 m from the ground to prevent destruction by elephants and, as a consequence, water levels could not be monitored after piezometers were submerged by flooding. Water levels in the piezometers were measured (logistics allowing) weekly using a tape measure with a sounding device.

Direct Measurements of Infiltration Rates

The large calculated lateral infiltration from the floodplain for the first two years (1997–1998) warranted experimental confirmation. Infiltration from the floodplain was therefore measured directly on two occasions in October and November 1999. Measurements took place at five transects across the littoral zone (Figure 1), oriented perpendicular to the shore. At each transect, point infiltration rates were measured at distances of 0.5, 1, 1.5, 2, 3, 4, 6, 8, and 10 meters from land. Water depths on the order
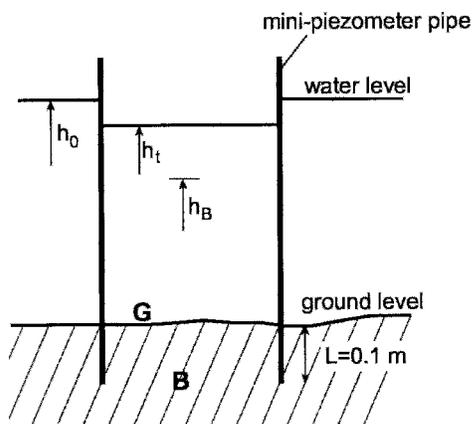
Figure 4. Schematic of a mini-piezometer used for direct measurements of point infiltration rates. Values of water levels and hydraulic heads h_t, h_0, and h_B measured with respect to an arbitrary reference level.

of several centimeters prevented the use of traditional "drum" type seepage meters as described by Lee (1977). Instead, infiltration was measured using mini-piezometers. The mini-piezometer was simply a PVC pipe of 0.10-m inner diameter (cross-section area $A = 0.0078$ m^2) and length 0.30–0.70 m (Figure 4). The pipe was inserted into the ground to a depth $L = 0.1$ m. At the beginning of a measurement ($t = 0$), water level inside the pipe was set at a level corresponding to water level outside of the pipe (h_0). Infiltration occurring inside the pipe caused gradual lowering of pipe water level. Water level in the pipe (h_t) was measured at various times t (every 2 hours over a 24-hour period). Instantaneous infiltration q_t inside the piezometer pipe is driven by a difference in hydraulic head between the bottom of the pipe (i.e., h_B at point B, Figure 4) and at the ground surface in the pipe (i.e., h_t at point G, Figure 4). It was assumed that h_B did not change during the experiment, while h_t corresponded to the actual water level in the pipe. Under such conditions, water level in the pipe is described by a combination of mass balance and Darcy equation:

$$\frac{dh}{dt} = k\frac{h_t - h_B}{L} \qquad (2)$$

where k is hydraulic conductivity of sediment inside the pipe.

Equation 2 (partial differential equation) solved by analytical methods under initial condition of h_t for $t = 0$ being equal to h_0, yields:

$$h_t = h_B + (h_0 - h_B)e^{-\frac{k}{L}t} \qquad (3)$$

Equation 3 is a function of the form: $h_t = f(t)$ with four parameters: L, h_0, h_B and k. Parameters L and h_0 characterize geometry of the instrument, and were

measured *a priori*. Measured pairs of h_t and t were used to determine values of parameters h_B and k. Since the function described by Equation 3 is non-linear, values of parameters h_B and k were determined using an optimization routine (an MS Excel function), which adjusted their values so the difference between measured h_t and that calculated from Equation 3 was minimized. Actual infiltration rate was the calculated considering that it takes place under condition of $h_t = h_0$:

$$I = k\frac{h_0 - h_B}{L}A \qquad (4)$$

The method did not account for open water evaporation taking place from within the pipes. Also, a distinction could not be made between infiltration contributing to deeper ground water and that supplying transpiration demand of aquatic macrophytes, rooted in shallow sediment. However, the infiltration values obtained in most of the measurement sites were very high (up to 42 cm·d^{-1}), by far exceeding open water evaporation during the measurement period (0.6–1.0 cm·d^{-1}). Considering the aim of the exercise (i.e., qualitative confirmation of the high infiltration rates obtained from water balance), the effects of evaporation (open water and macrophytes) were considered negligible and were not corrected.

RESULTS

General Patterns

During each studied year, the flood arrived at the end of May-beginning of June in the study area and lasted for 91–175 days (Table 1). The inflow to the floodplain had a similar pattern for the three studied years (Figure 2). Inflow increased rapidly after arrival of the flood, and the maximum inflow occurred within the first 30 days of flooding (end of June). Subsequently came a gradual, exponential-like decline in inflow. Water levels in the floodplain rose fast during the first 30 days of the flood, and this was accompanied by large increase in storage (high ΔS values in Figure 5). Unlike the inflow, however, after the initial rise, water levels stabilized for a period of 1–2 months (July–August). A rapid drop of water levels occurred at the end of the flood (i.e., in August–December) (Figure 2), which translates into decrease in floodplain storage (negative values of ΔS in Figure 5).

The total inflow varied between 0.49 and 1.42 million m^3 for the three seasons (Table 1). During the peak of the flood, the maximum depth of water in the floodplain was about 2 m and the mean depth 0.15–0.3 m, depending on the extent of

Table 1. Characteristics of flooding in the studied floodplain.

		1997	1998	1999
Total inflow	[m^3]	1 387 800	494 100	1 422 600
Duration of flooding	[d]	164	91	175
Mean flooded area	[m^2]	151 000	89 000	134 000
Mean floodplain volume	[m^3]	43 000	14 000	34 000
Mean floodplain water depth	[m]	0.28	0.16	0.25
Mean retention time	[d]	5.2	2.5	3.6

inundation. The inflow to the floodplain was large compared to the volume, and the mean retention time is calculated to be between 2 and 5 days for the years studied.

Infiltration Calculated from the Water Balance

On an annual basis, 88–91% of the water flowing into the floodplain infiltrated into the ground (Table 2). The infiltration was on the order of 4.7–9.7 m per season, or on average 4.6–5.4 cm·d^{-1} expressed over the actual flooded area.

The infiltration rate changed significantly throughout the flood season (Figure 5) and followed the general pattern of the inflow. At the arrival of the flood, infiltration was rapid, and later, the rate gradually decreased. During the initial rapid infiltration phase, rates as high as 1.74 m in 10 days were calculated.

The sensitivity analysis reveals (Figure 6) that eventual errors in evaporation or floodplain storage variables have little influence on the calculated total annual infiltration or on its temporal variability. Somewhat extreme assumption of 50% error in input variables causes only a 10% difference in calculated infiltration values. More conservative assumption of 20% error results in a difference in infiltration on the order of 3–4%.

Ground-Water-Table Fluctuations

The observed ground-water-table fluctuations are clearly related to flooding, and there is very little or no influence of rains. The magnitude and character of ground-water-table fluctuations depend on the distance from the perimeter of the inundated area. Within the inundated area, a rapid rise of the ground-water table with a rate of 1–1.5 m·d^{-1} occurred immediately after the onset of inundation (e.g., piezometer P2 in June 1997, Figure 7). Just before the flood arrived, the levels were approximately 3, 4, and 5 m below ground for the 1997, 1998, and 1999, respectively (P2 in Figure 7). The unsaturated volume under the inundated area was thus filled up in a few days. Further away from inundated area, the ground-water rise was less pronounced (piezometers P1, G and F, Figure 7). Water-level rise in piezometer G was approximately 3 m in 1997 when flood extended to approximately 20 m from it, but only 0.4 m in 1998 when flood stopped 250 m away. In piezometer F, located at a distance of about 400 m from the shoreline of 1997 flood, the rise in ground-water level during that year's flood was only 0.20 m, and the highest ground-water-table position was recorded in September, about three months after arrival of the water to the floodplain (Figure 7). The smaller flood of 1998, which reached 600 m from piezometer F, had no effect on ground water in that piezometer; a steady decline was recorded during that whole year.

Lateral Ground-Water Flow

The fluctuations of ground-water table (Figure 7) indicate that part of infiltrating water is removed
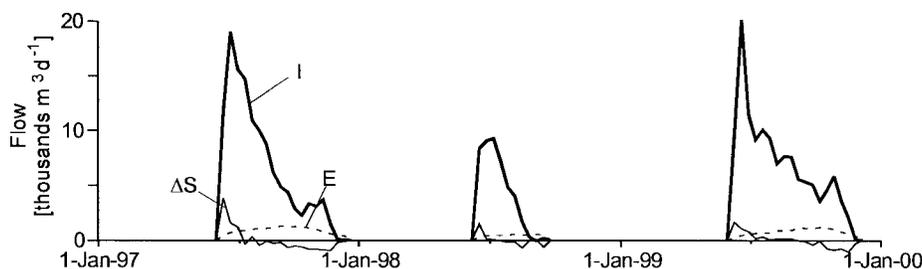

Figure 5. Elements of water balance of the Phelo's floodplain. *I* – infiltration, *E* – evaporation, *ΔS* – change in floodplain storage (negative values indicate reduction in floodplain storage).

WETLANDS, Volume 26, No. 3, 2006

Table 2. Water balance for the studied ÿ¢§floodplain.

			1997	1998	1999
Inflow	total	[m^3]	1 388 000	494 000	1422 000
	average daily	[cm·d^{-1}]	5.2	5.7	6.0
Evaporation	total	[m^3]	164 500	45 800	142 600
	average daily	[cm·d^{-1}]	0.6	0.5	0.6
Infiltration	total	[m^3]	1 223 300	448 300	1 279 000
	total[a]	[cm]	743	468	975
	average daily	[cm·d^{-1}]	4.6	5.2	5.4
	maximum	[cm/10 days]	114	111	174
Infiltration/inflow ratio		[–]	0.88	0.91	0.90
Infiltration/evaporation ratio		[–]	7.4	9.8	9.0

[a] calculated over the time-varying area of water surface.

from the floodplain by lateral ground-water flow towards surrounding drylands. The amount of water transferred out of the inundated area by lateral ground-water flow can be calculated by subtracting the (assessed) pre-inundation pore volume of vadose zone under the inundated area from the total annual infiltration (Table 3). The calculations reveal that the lateral ground-water flow toward the surrounding dryland accommodated 72–85% of the total seasonal infiltration.

Measured Infiltration Rates

Direct measurements of infiltration revealed point infiltration rates reaching 42 cm·d^{-1}. Infiltration takes place within a narrow littoral zone, and there is a progressive increase towards the shore (Figure 8), with 75% of the infiltration occurring within the 0–2 m band. The average of the five measured transects in October 1999 was 0.416 m^3·d^{-1}·m, which if extrapolated across the entire shoreline length, gives a total infiltration of 2247 m^3·d^{-1}. The total infiltration value, obtained in an analogous manner for the November experiment was 1768 m^3·d^{-1}. These values are lower but still within the same order of magnitude as the values of 5584 m^3·d^{-1} and 3690 m^3·d^{-1}, respectively, calculated from the water balance for the periods the infiltration measurements were made. There is
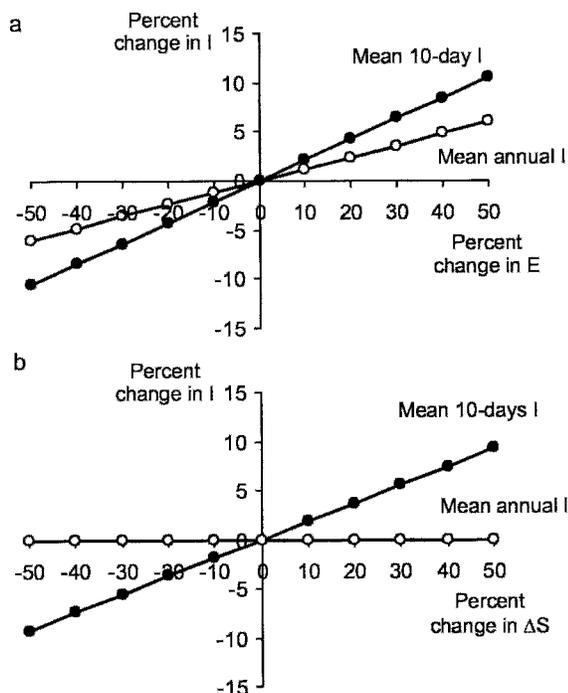

Figure 6. Sensitivity analysis. Lines represent change in infiltration (I) compared to original values, when calculated with −50% to +50% change in (a) evaporation E (b) floodplain storage ΔS.
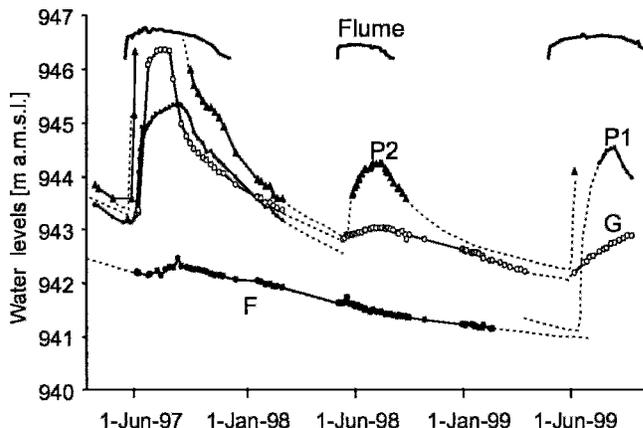

Figure 7. Ground-water-table fluctuations at piezometers and surface water levels at flume. F, G, P1 and P2 are piezometer designations. Location of piezometers shown in Figure 1. Dashed line represents interpreted levels.

Table 3. Assessment of the lateral ground-water outflow from the inundated area.

Year			1997	1998	1999
Maximum extent of the flooded area	A	[m^2]	203 000	103 000	145 000
Pre-flood ground-water-table depth	h	[m]	3	4	5
Porosity	n	[–]	0.3	0.3	0.3
First phase infiltration	I_1	[m^3]	182 700	123 600	217 500
Observed annual infiltration volume	I	[m^3]	1 223 300	448 300	1 279 900
Lateral groundwater outflow ($I–I_1$	I_2	[m^3]	1040600	324700	1062400
Lateral gw outflow as % of total infiltration		[%]	85	72	83
Lateral gw outflow as % of sum of total infiltration and water surface evaporation		[%]	75	65	75

a considerable variability among the sites that may explain the discrepancy (Figure 8).

INTERPRETATION AND DISCUSSION

Factors Affecting Magnitude and Variation of Infiltration

The measurements and calculations presented above reveal that infiltration is the dominant process responsible for flood water loss from the studied floodplain. The observed variations in ground-water-table level (Figure 7) suggest that the process of infiltration takes place in two phases (Figure 9). The first phase (Figure 9a) can be depicted as occurring at the propagating face of the flood and takes the form of vertical percolation of water through the vadose zone, probably analogous to Green-Ampt infiltration (Maidment 1992). Infiltration during this phase is fast because it is controlled
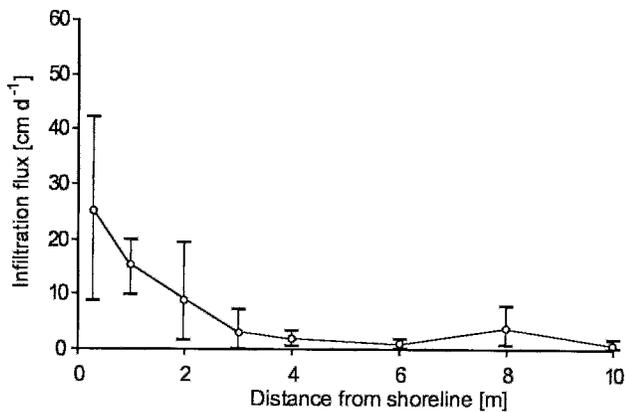

Figure 8. Infiltration flux. Mean and range measured by mini-piezometers at five different locations (shown in Figure 1) in November 1999.
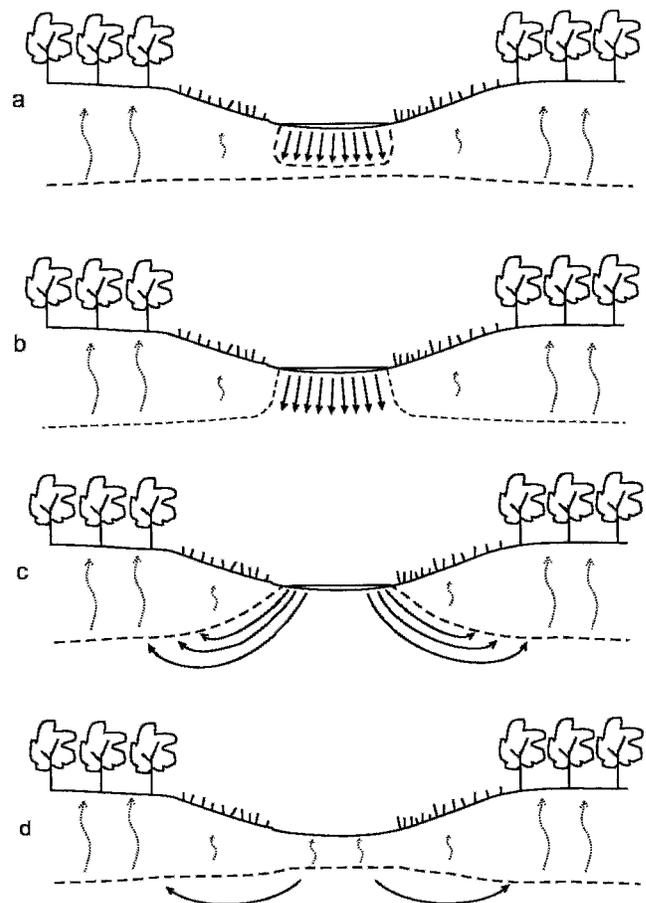

Figure 9. Schematic plot of interactions between surface water and ground water in the studied floodplain: (a) first phase infiltration (June), (b) and (c) second phase infiltration (July–September), (d) ground-water behaviour after flood cessation (October and later, depending on duration of inundation). Dotted lines represent evapotranspiration. Dashed line represents ground-water table, arrows represent ground-water flow directions. Density of the arrows indicates ground-water flux.

by vertical hydraulic conductivity of the floodplain bed and vadose zone, which are high in the studied floodplain. After some time, the percolation front connects with the shallow ground-water table, and the second phase begins. During that phase (Figure 9b–c), infiltration can be depicted as controlled not only by the properties of the vadose zone but also by conditions defining transfer of ground water from beneath the flooded area toward its surroundings.

This two-phase infiltration process is reflected in the infiltration rates obtained from the water balance: the high infiltration rates observed during the first 30 days of flooding (June) result mainly from the first phase, occurring during the expansion of the flood. However, because the flood expands gradually, the slower, second phase infiltration also contributes to the calculated rates during that period. The decline in infiltration rates observed after the first 30 days of flood (July and later), however, reflects the lateral ground-water-flow-controlled second phase infiltration only.

The first phase occurs typically during 1–3 days after inundation, and thus, its local rates are higher than those obtained from the 10–day water balance and integrate both the first and the second phase infiltration in a situation of expanding flood. Ground-water-table observations from Phelo's Floodplain suggest first phase infiltration rates of approximately 1.5 m·d^{-1} and more. Such high values are rather unusual in wetlands, as floodplains are typically lined with low permeability deposits that limit infiltration. Generally, the values of hydraulic conductivity of floodplain soils fall between $1·10^{-10}$ and $1·10^{-5}$ m·s^{-1} (Mitsch and Gosselink 2000). The Okavango River, however, drains a catchment covered with highly weathered quartzitic Kalahari sands and carries very little fines (McCarthy et al. 1998). As a result, the Okavango Delta is built of permeable sands, and the clogged layer is not present in the floodplains. Additionally, fires are frequent in the seasonal floodplains of the Okavango Delta (Heinl et al. 2004), preventing the build-up of peat that could otherwise reduce the infiltration capacity of floodplain soil. Values of infiltration capacities of between $4.6·10^{-4}$ and $1.2·10^{-3}$ m·s^{-1} (Boring and Björkvald 1999) and hydraulic conductivities of floodplain strata between $1.2·10^{-4}$ and $3.5·10^{-4}$ m·s^{-1} (Obakeng and Gieske 1997) confirm that the high observed values of the first phase infiltration rates are realistic.

During the second phase of infiltration, infiltration rates are controlled by ground-water drainage, and the calculations (Table 3) revealed that up to 85% of the annual infiltration occurred during this phase. At the onset of the second phase infiltration (July), ground-water gradients in the vicinity of the floodplain are steep and drive relatively large lateral ground-water flux, and thus relatively large infiltration (Figure 9b). As a consequence of lateral ground-water flow, the ground-water table around the floodplain gradually rises, causing a reduction of ground-water gradients and thus reduction of infiltration (Figure 9c). During the period when the second phase of infiltration becomes dominant (July–September in 1998 and July–December in 1997 and 1999), infiltration rates averaged over the inundated area were generally below 9 cm·d^{-1}. However, our infiltration experiments showed that infiltration took place in a narrow zone close to the shore, with local rates on order of 9–42 cm·d^{-1} (Figure 8). The presence of higher infiltration rates in the littoral zone is a general pattern for inflow from surface waters to hydraulically connected shallow ground-water systems (e.g., Freeze and Cherry 1979, Winter 1999).

After cessation of the flood, during each year of the study, the ground-water table declined rapidly (Figure 7). Wolski and Savenije (2003) have shown, using a regional ground-water model, that due to a generally small regional topographic gradient (~1:3600), regional ground-water drainage in the central Okavango Delta could not exceed 0.1 cm·a^{-1}. Thus, the observed recession of the ground-water table is attributed to ground-water evaporation and transpirative uptake (both by floodplain vegetation made up of grasses and sedges and by dryland trees), and continuous ground-water transfer between floodplain and dryland in a local ground-water-flow system. Reversal of the ground-water gradient between floodplain and dryland has never been observed, neither in this study, nor at other sites in the Okavango Delta (e.g., McCarthy et al. 1991, Wolski and Savenije 2003, WRC 2003, Bauer 2004). Ground-water flow from floodplains toward drylands seems, therefore, to be a permanent and characteristic feature of the Okavango Delta, and the effect of bank storage defined as return flow toward the floodplain after drop in flood levels, is not present.

Comparison with Other Sites in Okavango and Other Wetland Systems

In this study, the calculated total infiltration accounted for 88–91% of inflowing water, and the mean daily infiltration rate varied between 4.6 and 5.4 cm·d^{-1}. These values are comparable to values obtained during earlier studies in the Okavango. At Beacon Island site (Figure 1) infiltration was 72–

84% of the net inflow or on average 1.3–1.8 cm·d^{-1} (Dinçer et al. 1976); in the Gumare channel (Figure 1), mean daily infiltration rate was 7.7 cm·d^{-1} (Petermann et al. 1988) and constituted 92% of the transmission loss.

The values of infiltration measured and calculated for the Phelo's Floodplain exceed typical values observed in other recharge wetlands and floodplain wetlands. Mitsch and Gosselink (2000) provided water balance for several wetlands, and for those with a significant ground-water recharge function, ground-water recharge (which we consider to be equal to infiltration) falls between 1 and 28 cm·a^{-1}, which represents 2–30% of the combined evaporation and ground-water recharge loss in those wetlands. In the Nigerian Hadejia-Nguru wetlands, characterized by a similar climate to that of Okavango, a seasonal flood-pulse of 4 months caused ground-water recharge of 50 cm·a^{-1}, which was 51% of the combined evaporation and recharge loss in that wetland (Goes 1999, Thompson and Polet 2000). The high infiltration values for Phelo's Floodplain are, however, much lower than infiltration rates observed in ephemeral rivers, which typically fall between 35 and 520 cm·d^{-1} (Lerner et al. 1990). Obviously, rates for ephemeral rivers reflect a situation where there is no hydraulic link between surface water and ground water, and infiltration takes place as a Green-Ampt process during relatively short time periods, and thus the rates are extremely high. In seasonal floodplains, however, flood-water infiltration rates are normally limited by low hydraulic conductivity of the floodplain bed, and in places, infiltration might not play any role. For example, during a large flood in the Murray River floodplain in Australia, diffuse vertical recharge of floodwater to ground water was shown to be of little importance (Jolly et al. 1994, Lamontagne et al. 2005). In the case of permeable floodplain deposits, total infiltration corresponds to the depth of vadose zone before inundation and to the capacity of the shallow ground-water aquifer to carry ground water out of the floodplain. The high infiltration at Phelo's Floodplain, as compared to Hadejia-Nguru, seems to result from the difference in the role of the last factor (i.e., lateral ground-water drainage). In the Hadejia-Nguru, lateral ground-water drainage was limited, as it occurred at the perimeter of a relatively large flooded area. In contrast, due to the large area of surrounding dryland and the small size of Phelo's Floodplain, lateral ground-water drainage was very significant. An additional factor that affects the lateral ground-water drainage, and thus effectively increases infiltration in Phelo's Floodplain, is the presence of dryland vegetation taking up ground water for evapotranspiration. It is known that evapotranspirative uptake of ground water by riparian vegetation can cause an increase in infiltration rates (Sacks et al. 1992, Doss 1993, Winter and Rosenberry 1995). For example, in a prairie pothole described by Hayashi et al. (1998), as much as 50–75% of the combined (evaporation and ground-water recharge) water loss from the wetland was caused by transpiration-driven lateral ground-water flow.

Implications of High Infiltration for the Hydrology and Ecology of the System

Infiltration is not only a major mechanism of water loss from Phelo's Floodplain, but it seems that it in fact determines the amount of water flowing into it. Inflow to Phelo's Floodplain increases significantly at the onset of the flood. This results from an increasing water-level gradient between the feeding Boro River and Phelo's Floodplain, resulting from the arrival of the flood wave in the Boro River. The decline of inflow observed after the first 30 days of flooding occurs, however, while water levels in both the Boro and on Phelo's Floodplain remain stable. The decline in inflow thus cannot be a reflection of limitation in flood water supply to the floodplain or falling water levels in the Boro River. Since inflow and infiltration change concurrently, the decline in inflow must, therefore, result from the decline in infiltration. In this way, the infiltration effectively determines the amount of water flowing into the floodplain.

The infiltrating and laterally transported water supports riverine forests on the dryland fringes in the Okavango Delta. These forests occur not only along rivers and other permanent waters but also along seasonal floodplains (SMEC 1989, Ringrose 2003), vary in width from 20 m to 200 m, and cover 1500 km^2 (Ringrose 2003, Wolski and Gumbricht 2003). The riparian vegetation forms an important Okavango Delta habitat, used by a wide variety of animals (e.g., elephants) and birds for shelter and feeding and adds to its aesthetic value for tourism.

Okavango waters are generally nutrient-poor and are often classified as oligo- to mesotrophic (Cronberg et al. 1996, Wolski et al. 2005a). Yet, surface water is an important source of nutrients in the seasonal floodplains (Krah et al. 2005). The high infiltration rates, as shown above, drive inflow to the floodplain and thus increase the pool of nutrients available in a floodplain, as compared to a situation where there is evaporation-driven inflow only. Some

of the nutrients escape from the floodplain with infiltrating water (Wolski et al. 2005a). It is possible, however, that high infiltration does increase the amount of nutrients available for floodplain vegetation. This could be mainly through the increase in the depth of the aerobic layer in the floodplain substratum, which results in nitrification of ammonium nitrogen and sequestration of nitrate nitrogen by plants and microbes. Examples of such processes are known from rivers, where ripple and pool sequences create downwelling and upwelling sections in the hyporheic zone, which differ significantly in biogeochemistry (Brunke and Gonser 1997, Mermillod-Blondin et al. 2000). Work done so far on nutrient balance in seasonal floodplains in the Okavango Delta (Cronberg et al. 1996, Mubyana et al. 2003, Krah et al. 2005, Wolski et al. 2005a) does not, however, take these potentially important processes into account.

Additionally, the large lateral ground-water drainage is a mechanism causing effective immobilization of dissolved salts in the system. The Okavango Delta is essentially a closed (endorheic) system, where all the water is ultimately lost by evaporation and transpiration. In spite of that, the Okavango Delta remains a fresh water body due to the process of trapping the salts under islands, described in detail by McCarthy et al. (1991), McCarthy et al. (1998), and Bauer (2004). In this process, the evapotranspirative uptake of ground water by dryland vegetation creates a permanent cone of depression in island ground water, effectively preventing the movement of inorganic ions left in the ground water after evaporative uptake. The large infiltration and lateral ground-water movement detected in this study is therefore a prerequisite of that process. Additionally, it is possible that the process is also responsible for removal of some of the nutrients (N and P) from the floodplains and their immobilization under the islands (Wolski et al. 2005a). This is potentially important in this generally nutrient-deficient system.

Another important consequence of high infiltration rates is their potential effect on the process of mobilization and redistribution of chemicals and nutrients from the surface by flood water. In floodplains with low infiltration rates, inorganic minerals (capillary precipitates and atmospheric deposits) and nutrients (mineralized detritus) remaining after the previous flood can diffuse upward to surface water from the surficial layer of the soil of a certain depth. In a situation of high infiltration, the thickness of this contributing layer is reduced, as such diffusion has to act against the downward convective movement of water through the interstitial spaces of the floodplain substratum. The importance of this process in redistribution of minerals and nutrients in the Okavango Delta has not been addressed so far.

SUMMARY AND CONCLUSIONS

The results of the study of water balance of a seasonally inundated floodplain presented here reveal extremely large infiltration rates and volumes. The interaction between surface water and ground water is exclusively one-directional (i.e., no exfiltration or return flow was recorded), and infiltration effectively determines inflow of water and thus nutrients and minerals to the floodplain. The combination of these characteristics, and in particular the high infiltration rates, are rather unusual in recharge wetlands.

The high infiltration rates are responsible for the removal of solutes from the floodplain. They determine the nutrient budget of the floodplain, probably strongly affecting nutrient distribution and lateral movement during flood propagation.

The large lateral ground-water flow indicates that the riparian woodland is functionally dependent on flood water. This process has to be taken into account in assessments of environmental impacts of various actions that may reduce the extent or duration of flooding in the Okavango Delta. Modifications of hydroperiod will not only have a direct impact on the aquatic component of the Okavango Delta ecosystem but will also affect the large areas of riparian woodlands. The environmental costs of such proposed developments and similar actions would be considerably higher than previously anticipated. Additionally, actions that might affect the riparian woodland on a large scale (e.g., clearing for agriculture or destruction by large population of elephants) have large implications for water and salt balance in the system.

In the previous hydrologic models of the Okavango Delta (Dinçer et al. 1987, Scudder et al. 1993, Gieske 1997), infiltration and lateral ground-water flows were not incorporated or were very simplified. This study reveals that these two processes are quantitatively very important, at least in some parts of the system, and thus their dynamics and volumes of water involved have to be properly represented in hydrologic models. The more recent, distributed models (Bauer 2004, Jacobsen et al. 2005) simulate processes of surface water and ground water implicitly, while the conceptual (reservoir) model of Wolski et al. (2005b) simulates the surface-water ground-water relationship explicitly. In this frame-

work, this paper provides a quantitative basis for parameterization, calibration, and verification of the surface water ground-water interaction element of these models.

LITERATURE CITED

Bauer, P. 2004. Flooding and salt transport in the Okavango Delta, Botswana: key issues for sustainable wetland management. Ph. D. Dissertation, ETH Zurich, Zurich, Switzerland.

Boring, M. and L. Björkvald. 1999. A minor field study of the infiltration rate on a floodplain in the Okavango Delta, Botswana. Research Report. Göteborg University, Sweden and Harry Oppenheimer Okavango Research Centre, University of Botswana, Botswana.

Brunke, M. and T. Gonser. 1997. The ecological significance of exchange processes between rivers and groundwater. Freshwater Biology 37:1–35.

Choi, J. and J. W. Harvey. 2000. Quantifying time-varying ground-water discharge and recharge in wetlands of the northern Florida Everglades. Wetlands 20:500–511.

Cronberg, G., A. Gieske, E. Martins, J. Prince-Nengu, and I. Stenstrom. 1996. Major ion chemistry, plankton, and bacterial assemblages of the Jao/Boro River, Okavango Delta, Botswana: the swamps and flood plains. Archiv für Hydrobiologie. Supplementband. Monographische Beitraege 3:335–407.

Dinçer, T., S. Child, and B. Khupe. 1987. A simple mathematical model of a complex hydrologic system - Okavango Swamp, Botswana. Journal of Hydrology 93:41–65.

Dinçer, T., H. H. Heemstra, and D. B. Kraatz. 1976. The study of hydrological conditions in an experimental area in the seasonal swamp. Technical Note No. 20. UNDP/FAO, BOT/71/706, Gaborone, Botswana.

Doorenbos, J. and W. O. Pruitt. 1984. Crop water requirements. Irrigation and Drainage Paper No. 24. FAO, Rome, Italy.

Doss, P. K. 1993. The nature and dynamics of water table in a system of non-tidal, freshwater coastal wetlands. Journal of Hydrology 141:107–126.

Ellery, K. and W. Ellery. 1997. Plants of the Okavango Delta. A Field Guide. Tsaro Publishers, Durban, South Africa.

Ellery, W. N., K. Ellery, and T. S. McCarthy. 1993. Plant distribution in islands of the Okavango Delta, Botswana: determinants and feedback interactions. African Journal of Ecology 31:118–134.

Freeze, R. A. and J. A. Cherry. 1979. Groundwater. Prentice-Hall, Engelwood Cliffs, NJ, USA.

Gieske, A. 1997. Modelling outflow from the Jao/Boro River system in the Okavango Delta, Botswana. Journal of Hydrology 193:214–239.

Goes, B. J. M. 1999. Estimate of shallow groundwater recharge in the Hadejia-Nguru Wetlands, semi-arid northeastern Nigeria. Hydrogeology Journal 7:294–304.

Gumbricht, T., J. McCarthy, and T. S. McCarthy. 2004. Channels, wetlands and islands in the Okavango Delta, Botswana, and their relation to hydrological and sedimentological processes. Earth Surface Processes and Landforms 29:15–29.

Harrington, G. A., P. G. Cook, and A. L. Herczeg. 2002. Spatial and temporal variability of ground water recharge in central Australia: a tracer approach. Ground Water 40:518–528.

Harvey, J. W., J. Choi, and R. H. Mooney. 2000. Hydrologic interactions between surface water and ground water in Taylor Slough, Everglades National Park. p. 22–24, *In* J. R. Eggleston (ed.) U.S. Geological Survey Program on the South Florida Ecosystem: 2000 proceedings. U.S. Geological Survey Open-File Report 00–449, USGS, Denver, CL, USA.

Harvey, J. W., S. L. Krupa, and J. M. Krest. 2004. Ground water recharge and discharge in the Central Everglades. Ground Water 42:1090–1102.

Hayashi, M., G. van der Kamp, and D. L. Rudolph. 1998. Water and solute transfer between a prairie wetland and adjacent uplands, 1. Water balance. Journal of Hydrology 207:42–55.

Heinl, M., J. Sliva, and B. Tacheba. 2004. Vegetation changes after single fire-events in the Okavango Delta wetland, Botswana. South African Journal of Botany [Online] 70:695–704.

Hoberg, P., M. Lindholm, L. Ramberg, and D. O. Hessen. 2002. Aquatic food web dynamics on a floodplain in the Okavango Delta, Botswana. Hydrobiologia 470:23–30.

Hughes, F. M. R. 1990. The influence of flooding regimes on forest distribution and composition in the Tana River floodplain, Kenya. Journal of Applied Ecology 27:475–491.

Jacobsen, T., A. McDonald, and H. Enggrob. 2005. Integrated Hydrological Model. Okavango Delta Management Plan, Department of Water Affairs, Gaborone, Botswana.

Jolly, I. D., G. R. Walker, and K. A. Narayan. 1994. Floodwater recharge process in the Chowilla Anabranch system, South Australia. Australian Journal of Soil Research 32:417–435.

Jones, J. B. and P. J. Mulholland. 2000. Streams and Ground Waters. Academic Press, San Diego, CA, USA.

Kgathi, D. L., G. Mmopelwa, and K. Mosepele. 2005. Natural resources assessment in the Okavango Delta, Botswana: case studies of some key resources. Natural Resources Forum 29:70–81.

Krah, M., T. C. McCarthy, P. Huntsman-Mapila, P. Wolski, and K. Sethebe. 2005. Nutrient transport with water, from soil surfaces and local aerosol deposition into the landlocked Okavango Delta, Botswana - a floodplain case study. Wetlands Ecology & Management (in print).

LaBaugh, J. W., T. C. Winter, V. A. Adomaitis, and G. A. Swanson. 1987. Hydrology and chemistry of selected prairie wetlands in the Cottonwood Lake area, Stutsman County, North Dakota. U.S. Geological Survey Professional Paper 1431, USGS, Denver, CL, USA.

Lamontagne, S., F. W. Leaney, and A. L. Herczeg. 2005. Groundwater-surface water interactions in a large semi-arid floodplain: implications for salinity management. Hydrological Processes 19:3063–3080.

Lee, D. R. 1977. A device for measuring seepage flux in lakes and estuaries. Limnology and Oceanography 22:140–147.

Lerner, D. N., A. S. Issar, and I. Simmers. 1990. Groundwater Recharge. A guide to understanding and estimating natural recharge: International Contributions to Hydrogeology, vol. 8. Heise, Hannover, Germany.

Maidment, D. R. 1992. Handbook of Hydrology. McGraw-Hill, New York, NY, USA.

Martí, E., S. G. Fisher, J. D. Schade, and N. B. Grimm. 2000. Flood frequency and stream-riparian linkages in arid lands. p. 111–136, *In* J. B. Jones and P. J. Mulholland (eds.) Streams and Ground Waters. Academic Press, San Diego, CA, USA.

Mbaiwa, J. E. 2003. The socio-economic and environmental impacts of tourism development on the Okavango Delta, north-western Botswana. Journal of Arid Environments 54:447–467.

McCarthy, J., T. Gumbricht, T. S. McCarthy, P. E. Frost, K. Wessels, and F. Seidel. 2004. Flooding patterns in the Okavango Wetland in Botswana between 1972 and 2000. Ambio 7:453–457.

McCarthy, T. S., M. Barry, A. Bloem, W. N. Ellery, H. Heister, C. L. Merry, H. Rother, and H. Sternberg. 1997. The gradient of the Okavango fan, Botswana, and its sedimentological and tectonic implications. Journal of African Earth Sciences 24:65–78.

McCarthy, T. S., A. Bloem, and P. A. Larkin. 1998. Observations on the hydrology and geohydrology of the Okavango Delta. South African Journal of Geology 101:101–117.

McCarthy, T. S., J. R. McIver, and B. T. Verhagen. 1991. Groundwater evolution, chemical sedimentation and carbonate brine formation on an island in the Okavango Delta swamp, Botswana. Applied Geochemistry 6:577–595.

Mermillod-Blondin, F., M. Creuze des Chantelliers, P. Marmonier, and M. Dole-Olivier. 2000. Distribution of solutes, microbes and invertabrates in river sediments along a riffle-pool-riffle sequence. Freshwater Biology 44:255–269.

Meyer, T. 1999. Ecological mappings in the research area of the Harry Oppenheimer Okavango Research Centre, Okavango Delta, Botswana. M. Sc. Thesis. Anhalt Technical University, Anhalt, Germany.

Mitsch, W. J. and J. G. Gosselink. 2000. Wetlands. John Wiley & Sons, New York, NY, USA.

Mladenov, N., D. McKnight, P. Wolski, and L. Ramberg. 2005. Effects of annual flooding on dissolved organic carbon dynamics within a pristine wetland, the Okavango Delta, Botswana. Wetlands 25:622–638.

Mubyana, T., M. Krah, O. Totolo, and M. Bonyongo. 2003. Influence of seasonal flooding on soil total nitrogen, organic phosphorus and microbial populations in the Okavango Delta, Botswana. Journal of Arid Environments 54:359–369.

Obakeng, O. and A. Gieske. 1997. Hydraulic conductivity and transmissivity of a water-table aquifer in the Boro River system, Okavango Delta. Department of Geological Survey, Lobatse, Botswana.

Petermann, T., E. de Nooy, and H. Bendsen. 1988. Thaoge River Project. Evaluation Mission. Molapo Development Project, Department of Agriculture, Maun, Botswana.

Ringrose, S. 2003. Characterisation of riparian woodlands and their potential water loss in the distal Okavango Delta, Botswana. Applied Geography 23:281–302.

Sacks, L. A., J. S. Herman, L. F. Konikow, and A. L. Vela. 1992. Seasonal dynamics of groundwater-lake interactions at Doñana National Park, Spain. Journal of Hydrology 136:123–254.

Scudder, T., R. E. Manley, R. W. Coley, R. K. Davis, J. Green, G. W. Howard, S. W. Lawry, D. Martz, P. P. Rogers, A. R. D. Taylor, S. D. Turner, G. F. White, and E. P. Wright. 1993. The IUCN review of the Southern Okavango Integrated Water Development Project. IUCN, Gland, Switzerland.

SMEC. 1987. Study of open water evaporation in Botswana. Snowy Mountains Engineering Corporation, Ministry of Local Government and Lands, Gaborone, Botswana.

SMEC. 1989. Ecological zoning of the Okavango Delta. Snowy Mountains Engineering Corporation, Ministry of Local Government and Lands, Gaborone, Botswana.

Sophocleous, M. 2002. Interactions between groundwater and surface water: the state of science. Hydrogeology Journal 10:52–67.

Thompson, J. R. and G. Polet. 2000. Hydrology and land use in a sahelian floodplain wetland. Wetlands 20:639–659.

Tiner, R. W. 1999. Wetland Indicators: a Guide to Wetland Identification, Delineation, Classification, and Mapping. Lewis Publishers, Boca Raton, FL, USA.

Turton, A. R., P. J. Ashton, and T. E. Cloete. 2003. An introduction to the hydropolitical drivers in the Okavango River basin, p. 9–30, In A. R. Turton, P. J. Ashton, and T. E. Cloete (eds.) Transboundary Rivers, Sovereignty and Development: Hydropolitical Drivers in the Okavango River Basin. Green Cross International (GCI), Geneva, Switzerland.African Water Issues Research Unit (AWIRU), Pretoria, South Africa.

UNDP/FAO. 1977. Investigation of the Okavango Delta as a Primary Water Resource for Botswana. UNDP/FAO, DP/BOT/71/506, Gaborone, Botswana.

Winter, T. C. 1999. Relation of streams, lakes, and wetlands to groundwater flow systems. Hydrogeology Journal 7:28–45.

Winter, T. C., J. W. Harvey, O. L. Franke, and W. M. Alley. 1998. Ground water and surface water: a single resource. U.S. Geological Survey Circular 1139, USGS, Denver, CL, USA.

Winter, T. C. and D. O. Rosenberry. 1995. The interaction of groundwater with prairie pothole wetlands in Cottonwood Lake area, east-central North Dakota, 1979–1990. Wetlands 15:193–211.

Woessner, W. W. 2000. Stream and fluvial plain groundwater interactions: rescaling hydrogeological thought. Ground Water 38:423–429.

Wolski, P. and T. Gumbricht. 2003. Mapping hydrological units in the Okavango Delta. Water and Ecosystem Resources for Regional Development, EU ICA-4-CT-2001010040, Harry Oppenheimer Okavango Research Centre, Maun, Botswana.

Wolski, P., M. Murray-Hudson, P. Fernkvist, A. Lidén, P. Huntsman-Mapila, and L. Ramberg. 2005a. Islands in the Okavango Delta as sinks of water-borne nutrients. Botswana Notes and Records 37:253–263.

Wolski, P., H. H. S. Savenije, M. Murray-Hudson, and T. Gumbricht. 2005b. Modelling the hydrology of the Okavango Delta, Botswana. J. Hydrol. (in print).

Wolski, P. and H. H. S. Savenije. 2003. Update of conceptual hydrological model of the Delta. Water and Environmental Resources for Regional Development, EU ICA-4-CT-2001-10040, Harry Oppenheimer Okavango Research Centre, Maun, Botswana.

WRC. 2003. Maun Groundwater Development Project, Project Review. Water Resources Consultants, Department of Water Affairs, Gaborone, Botswana.